JCTC Journal of Chemical Theory and Computation

An Improved Self-Consistent-Charge Density-Functional Tight-Binding (SCC-DFTB) Set of Parameters for Simulation of Bulk and Molecular Systems Involving Titanium

Grygoriy Dolgonos,* Bálint Aradi, Ney H. Moreira, and Thomas Frauenheim

Bremen Center for Computational Materials Science, University of Bremen, Am Fallturm 1, 28359 Bremen, Germany

Received August 12, 2009

Abstract: A new self-consistent-charge density-functional tight-binding (SCC-DFTB) set of parameters for Ti−X pairs of elements (X = Ti, H, C, N, O, S) has been developed. The performance of this set has been tested with respect to TiO_2 bulk phases and small molecular systems. It has been found that the band structures, geometric parameters, and cohesive energies of rutile and anatase polymorphs are in good agreement with the reference DFT data and with experiment. Low-index rutile and anatase surfaces were also tested. For molecular systems, binding and atomization energies close to their DFT analogues have been achieved. Large errors, however, have been found for systems in high-spin states and/or having multireference character of their wave functions. The correct performance of SCC-DFTB for surface reactions has been demonstrated via the water splitting on anatase (001) surface. The current SCC-DFTB set is a suitable tool for future in-depth investigation of chemical processes occurring on the surfaces of TiO_2 polymorphs as well as for other processes of physicochemical interest.

1. Introduction

Among 3d transition metals, titanium is the second most abundant element after iron that occurs in the Earth's crust.[1] It has plenty of interesting physical and chemical properties (i.e., low density, high thermal and mechanical strength, insensitivity to corrosion) that makes it the metal of choice for the construction of jet engines of many airplanes, of tanks, and of autoclaves for chemical processing, or even to create lustrous and exotic jewelry. In addition, titanium and its alloys serve as excellent dental implants due to their biocompatibility and corrosion resistance as well as due to the strong attachment of the implant to the bone (osseointegration).[2,3] Titanium also plays an important role in catalysis as its compounds (Ziegler−Natta catalysts) serve as coordination centers upon polymerization of α-olefins leading to stereoregular products.[4]

The major technologically important titanium compound is titanium dioxide, which is mainly used as a white pigment in many products ranging from paint and paper to ceramics and toothpaste. Moreover, titanium dioxide has also been shown to exhibit unique characteristics[5] suitable for gas sensing,[6,7] solar cells,[8] water photolysis,[9] and photocatalytic decomposition of organic and inorganic pollutants.[10−12] Given these exciting applications, it becomes necessary not only to synthesize such solid-state and molecular systems but also to reliably model their properties at an appropriate size and time scale.

Apparently, on the theoretical side, we are still limited to using the main electronic structure theories—Hartree−Fock (HF) or density-functional (DFT) ones—as the usage of highly correlated methods for large periodic/molecular systems is not feasible. However, even within a DFT framework, the results may sometimes suffer from incomplete treatment of electron correlation leading to underestimation of band gaps of TiO_2 polymorphs (rutile and anatase)[13] or to incorrect treatment of weakly bound (hy-

* Corresponding author e-mail: grygoriy.dolgonos@bccms.uni-bremen.de.

10.1021/ct900422c
Published on Web 12/18/2009

drogen-bonded and van der Waals) molecular systems.[14,15] Nevertheless, DFT usually provides acceptable results for the ground-state properties, which are in better agreement with experiment than HF ones. On the other hand, DFT-quality results can be also achieved by applying an approximate self-consistent-charge density-functional tight-binding (SCC-DFTB) method[16,17] provided that the corresponding Hamiltonian and respective integral tables have been thoroughly derived and tested. Due to its tight-binding-like nature, this method allows one to gain up to 2 orders of magnitude in speed compared to standard DFT without a significant loss of accuracy.[18] Therefore, SCC-DFTB serves as a computationally efficient method to investigate electronic, structural, and energetic properties of both molecules and bulk periodic systems.

Formerly, a SCC-DFTB parametrization for the pairs of elements involving titanium and carbon, hydrogen, nitrogen, and oxygen was created.[19] This parametrization has been directed mainly toward molecular systems and complexes, and according to our benchmark results, is not fully applicable to periodic systems such as respective solids and related surfaces. The aim of the current work is to remedy this shortcoming and to develop a new, widely transferable, SCC-DFTB data basis, which could be applied for both molecular and periodic structures. Since the main interest is concentrated on simulation of TiO_2 systems, a special accent in parametrization has been made on the reproducibility of rutile and anatase bulk structures and surfaces. Additionally, we also developed parameters for titanium−sulfur interactions as sulfur is one of the elements of great importance for the photocatalytic applications of TiO_2.

This paper is organized as follows. Section 2 contains a brief overview of the SCC-DFTB formalism and the parametrization details as well as the details of the reference DFT methodology. In section 3, a validation of the newly derived SCC-DFTB parameters is presented, and the conclusions follow in section 4.

2. Computational Methodology

2.1. SCC-DFTB Method. The SCC-DFTB method is based on the second-order expansion of the Kohn−Sham total energy with respect to charge density fluctuations (for a more detailed description, see refs 16−18 and 20). In other words, the total energy expression includes not only the standard tight-binding (TB) "band structure" E_{BS} and short-range repulsive terms E_{rep}, but also an electrostatic-interaction term $E_2(n, \Delta n)$ that accounts for the charge fluctuations:

$$E_{tot} = E_{BS} + E_{rep} + E_2(n, \Delta n) = \sum_i^{occ} n_i \langle \psi_i | \hat{H}^0 | \psi_i \rangle + E_{rep} + \frac{1}{2} \sum_{a,b}^{M} \gamma_{ab} \Delta q_a \Delta q_b \quad (1)$$

The first term of eq 1 is the sum over the occupied electronic eigenstates ψ_i of the effective Kohn−Sham Hamiltonian $\hat{H}^0$, derived under the approximation that the initial electronic density of the many-atom system can be represented as a superposition of corresponding neutral atomic charge densities. The Hamiltonian $\hat{H}^0$ depends only on this properly chosen reference density. The second term E_{rep} accounts for the energy difference between the electronic part of the (SCC-)DFTB method and DFT for a given reference system and comprises a summation over the Coulombic and exchange double counting terms as well as the ion core−core repulsion. Finally, the second-order term $E_2(n, \Delta n)$ is represented by atomic charge fluctuations Δq_a and Δq_b (based on Mulliken charges) together with an analytical interpolating function γ_{ab}. This term becomes important for the systems bearing atoms with different electronegativities leading to the formation of covalent polar or ionic bonds.

Further, the SCC-DFTB method relies on the following assumptions:

1. Only valence electrons are treated explicitly.

2. Kohn−Sham orbitals are expanded within the LCAO approximation using minimal localized pseudoatomic Slater orbitals, which include the confinement harmonic potential $(r/r_0)^2$ for the orbital localization (where r_0 is called a "wave function confinement radius").

3. The effective one-electron Kohn−Sham potential of many-atom system is constructed using a superposition of unperturbed neutral (pseudo)atomic densities (obtained with PBE functional[21]) which are confined by an analogous $(r/r_0)^2$ potential (with r_0 as a "density confinement radius").

4. The nondiagonal Hamiltonian matrix elements are derived on the basis of a two-center approximation, whereas the diagonal elements correspond to the calculated atomic orbital energies.

5. The repulsive term is approximated as the sum over all pairs of atom−atom potentials, which in turn are determined as a difference between the SCC-DFTB electronic energy and DFT total energy as a function of interatomic distance for properly chosen reference systems.

The computational efficiency of the SCC-DFTB method originates from the use of tabulated values of Hamiltonian and overlap matrix elements over a large number of interatomic distances that allows one to obtain interpolated values at any distance and to skip the computationally intensive explicit evaluation of two-center integrals. In addition, repulsion profiles are validated to be transferable, leading to DFT-quality results for the ground-state properties of typical organic molecules and solid-state systems while retaining at the same time the speed of common semiempirical methods.[18]

2.2. SCC-DFTB Parametrization Procedure. The successful SCC-DFTB parametrization implies that the main properties of reference systems are well reproduced with respect to DFT. This can be achieved by adjusting the wave function and density confinement radii (see above) for a given element as well as by accurate construction of repulsion profiles for all Ti−X diatomic cases.

In our previous SCC-DFTB parametrization of zinc-related systems,[22] it was found that the density confinement radius plays a marginal role on the quality of the obtained parameters whereas the wave function confinement radius is mainly responsible for the quality of band structures for periodic systems. Therefore, we have used the previous[19] value of 14 bohr for the former parameter but have checked the influence of the latter one on the Ti hexagonal-close-

Table 1. Reference Molecular Systems and Cutoff Values Used To Generate Ti−X (X = Ti, C, H, N, O, S) Repulsion Profiles

Ti−X pair	reference system	cutoff value, bohr	shift of repulsion curve
Ti−Ti	(singlet) Ti_2	5.68	no
Ti−O	TiO_2	5.49	no
Ti−H	TiH_4	3.60	no
Ti−C	$Ti(CH_3)_4$	5.78	upward by 0.7 eV/bond
Ti−N	$Ti(NH_2)_4$	6.60	upward by 0.5 eV/bond
Ti−S	TiS_2	7.48	no

packed (hcp) band structure. Early investigations on the DFTB parametrization of first-row elements and hydrogen[17] suggested that the wave function confinement radius should be approximately 2 times larger than the covalent radius of a given element (although this rule is not absolute for other elements). Therefore, after varying the value of the wave function confinement radius from 3 to 5 bohr, we have observed the best Ti band-structure reproducibility at 4.3 bohr and used this value throughout this study. It should be noted that this value is however slightly larger than the previously chosen one of 3.6 bohr.[19]

In the case of other elements (C, H, N, O, S), we have employed the same initial atomic parameters as have been reported earlier.[16] This ensures the applicability and transferability of our newly derived parameters among different molecular and periodic structures.

Repulsion profiles for Ti−X (X = Ti, C, H, N, O, S) pairs were generated by fitting with cubic splines the difference of DFT total energy and the electronic DFTB energy versus distance upon stretching Ti−X bonds in simple reference molecules. Different Ti−X repulsion profiles are characterized by different cutoff values indicating the distance at which the repulsion energy approaches zero. Table 1 gives an overview of parametrization details used for the generation of Ti−X repulsion profiles. It should be noted that in some cases (cf. Table 1, Ti−N and Ti−C pairs) the repulsion curve has to be shifted toward higher energies to reduce the errors associated with significant overbinding of reference systems.

All the reported parameters (set name "tiorg") can be downloaded from the DFTB webpage (see http://www.dftb.org/parameters/download).

2.3. Reference DFT Calculations. For molecular systems, we have employed the same methodology as was originally proposed by Zheng et al.:[19] all potential-energy-surface scans as well as geometry optimizations were performed using the hybrid Becke's three-parameter exchange functional with the Lee−Yang−Parr correlation functional (B3LYP)[23−25] in conjunction with a mixed SDD+ basis set. This basis set consists of a Stuttgart/Dresden SDD[26,27] effective core potential and basis set for titanium and Pople-style double-ζ 6-31G(d)[28] basis set for other elements. All these calculations were performed using the Gaussian 03 program package.[29]

For periodic systems, we have performed DFT calculations using Perdew, Burke, and Ernzerhof (PBE)[21] functional with double-ζ basis set including polarization functions as implemented in the SIESTA code.[30,31] The Troullier−Martins[32,33] scheme was employed to generate two types of pseudopotentials assuming $3s^23p^63d^24s^2$ (PP I) and $3d^24s^2$ (PP II) valence electronic configurations for titanium atom. The valence electronic configuration of oxygen was always $2s^22p^4$ throughout this study. The *k*-point sampling was performed in the same manner as for the SCC-DFTB calculations (see below). In the case of anatase, we have also carried out reference DFT calculations using the screened Hartree−Fock hybrid exchange-correlation (HSE06) functional[34,35] with projector-augmented plane wave (PAW)[36,37] potentials and treating Ti 3p electrons as valence ones. These calculations were performed with the Vienna Ab initio Simulation Package (VASP 5.2)[38−41] using an energy cutoff of 420 eV.

2.4. SCC-DFTB Calculations. Single-point SCC-DFTB calculations and geometry optimizations were carried out with the DFTB+ program.[42,43] In the latter case, the conjugate gradient algorithm[44] with the maximum force component of 10^{-4} au was employed. Bulk titanium, rutile, and anatase structures were simulated with the 8 × 8 × 4, 4 × 4 × 8, and 10 × 10 × 4 Monkhorst−Pack[45] grids for *k*-point sampling, respectively. The optimal lattice parameters were obtained after looking for a minimum-energy value from numerous single-point calculations having different *c*/*a* ratios, volumes, and internal *u* (for TiO_2 polymorphs) parameters. The rutile and anatase surfaces were modeled on the basis of periodic slabs for supercells having vacuum regions (>120 Å) and one *k*-point along the surface-normal directions. Cohesive, atomization, and binding energies were computed as the energy difference with respect to individual spin-polarized fragments (atoms). The mio-set[16,17] SCC-DFTB diatomic pairs involving carbon, hydrogen, oxygen, nitrogen, and sulfur were employed throughout this study.

3. Results and Discussion

In the following, our current parametrization results for some model systems involving Ti−X (X = Ti, C, H, N, O, S) Slater−Koster pairs will be presented in comparison to previous SCC-DFTB parametrization of Zheng et al.,[19] to DFT, and to available experimental data.

3.1. Ti−Ti Interactions: Ti hcp Structure. As mentioned earlier in section 2.2, we have found the best SCC-DFTB band-structure representation of Ti hcp phase using a titanium wave function confinement radius of 4.3 bohr. The corresponding band structure is depicted in Figure 1 together with the reference GGA-DFT one. One can easily see that the most of SCC-DFTB bands are compressed in comparison to their DFT analogues while retaining their shape. Such a behavior is typical for the SCC-DFTB method due to the minimal basis set employed and is commonly observed in the case of other elements.[22]

The equilibrium geometric parameters together with cohesive energies of Ti hcp bulk phase obtained using different SCC-DFTB parametrization sets, using DFT, and taken from experiment are given in Table 2. As seen from these data, the SCC-DFTB parametrization set of Zheng et al.[19] leads to the much shorter values of lattice constants *a* and *c* (although the *c*/*a* ratio is quite accurate) as a result of the strong overbinding of the Ti hcp phase. This trend may indicate that there is not enough contribution from the repulsion Ti−Ti energy near equilibrium bulk values. With

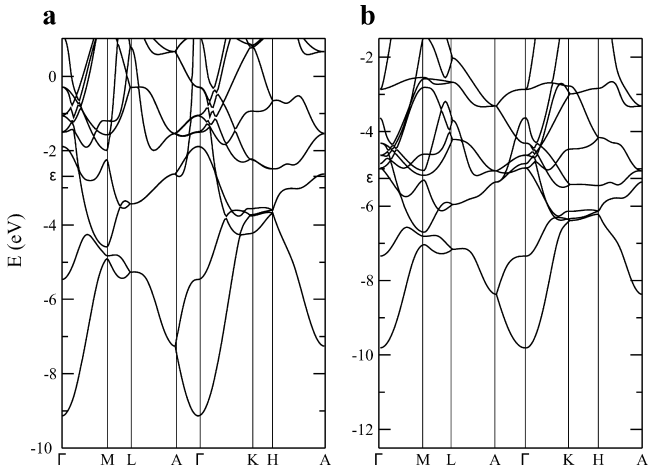

Figure 1. Titanium hcp band structures calculated with (a) GGA-DFT and (b) SCC-DFTB.

Table 2. Comparison of the Main Geometric and Energetic Parameters of Ti hcp Structure Calculated with SCC-DFTB and Obtained from Experiment

	SCC-DFTB		DFT			
parameter	set of Zheng et al.[19]	current set	LDA[a]	LDA[b]	PBE[b]	expt[c]
a, Å	2.380	2.998	2.866, 2.925	2.87	2.94	2.9508
c, Å	3.828	4.855	4.547, 4.666	4.526	4.642	4.6855
V, Å^3	18.78	37.80	32.34, 34.57	32.28	34.75	35.33
c/*a*	1.608	1.619	1.586, 1.595	1.577	1.579	1.588
E_{coh}, eV	11.58	6.49	6.42,[d] 5.20	6.70	5.87	4.85

[a] Linearized augmented plane-wave (LAPW) results of Lu et al.[47] using exchange-correlation potentials of Hedin−Lundqvist and exchange-only Xα (α = 2/3), respectively. [b] Full-potential LAPW results of da Silva et al.[84] [c] See ref 47 and references therein. For cohesive energy, see also ref 50. [d] Slightly smaller LDA value of 6.29 eV has been reported by Philipsen and Baerends[46] calculated using an experimental Ti hcp geometry.

the current SCC-DFTB set, we observe a much closer agreement of investigated properties with experiment: the *a* value lies within 0.06 Å to experiment or PBE, whereas the *c* value is more overestimated (by 0.21 and 0.17 Å to PBE and experiment, respectively). It should be noted however that the Ti hcp cohesive energy is now equal to 6.49 eV (and is overestimated by only 1.6 eV to experiment), which is comparable to DFT with local density approximation (LDA) values (6.29,[46] 6.42[47] eV). This result is quite satisfactory taking into account the general overestimation trend of the SCC-DFTB method itself.

3.2. Ti−O Interactions. Since the main aim of the current parametrization is to properly reproduce the properties of periodic systems involving titanium, the performance of this parametrization set for the two main TiO_2 polymorphs, rutile and anatase, and their surfaces is presented below.

3.2.1. Properties of Rutile and Its Low-Index Surfaces. The band structures of bulk rutile calculated with the current SCC-DFTB method and with GGA-DFT are shown in Figure 2. It is well-known that pure LDA and GGA functionals usually yield much smaller band gap values whereas hybrid functionals tend to overestimate this quantity.[13] In accord with this finding, our GGA results lead to band gap values of 1.7−2.0 eV, which are lower by more than 1 eV than the experimental one. Interestingly enough, in the case of the SCC-DFTB method we have found the minimal band gap at Γ of 3.13 eV that lies very close to the experimental value of 3.0 eV.[48,49] This presumably originates from the fortunate error cancellation associated with the minimal basis set used and other approximations of the SCC-DFTB method. However, the SCC-DFTB band structure differs significantly in the valence bands near the Γ-point from that obtained with DFT because of limitations of the SCC-DFTB method (cf. Figure 2c). This discrepancy cannot be cured by applying different wave function confinement radii for the oxygen atom nor by shifting the value of the oxygen 2s on-site energy.

Table 3 summarizes the main geometric and energetic characteristics of rutile bulk structure obtained with different DFT approaches and SCC-DFTB. We estimate the cohesive energy of rutile at 0 K by using the most recent CRC values[1] for the standard heats of formation of crystalline rutile and atomic oxygen as well as the cohesive energy of Ti hcp.[50] All less contributing terms such as thermal corrections and zero-point vibration energy of TiO_2 have been neglected. In general, all DFT methods overestimate the cohesive energy of rutile with hybrid functionals coming closer to the experimental value. Although SCC-DFTB also suffers from this deficiency, we managed to significantly reduce this overbinding trend in comparison to the previous set of Zheng et al.[19] and to bring down this property to 22.5 eV/TiO_2, which lies close to the PBE result of Lazzeri et al.[51] of 21.44 eV/TiO_2.

A comparison of rutile lattice parameters obtained with DFT and SCC-DFTB (see Table 3) indicates that, among GGA functionals, PBE generally reproduces the experimental values quite well whereas BLYP leads to larger *a* and *c* values. The previous SCC-DFTB set of Zheng et al.[19] gives too high a value of lattice constant *a*, while leading to the almost exact value of *c*. As a result, the corresponding *c*/*a* value is very low. The current SCC-DFTB parametrization overcomes this discrepancy and leads to a better agreement with experiment (though the *c* value is now only slightly overestimated). However, the bulk modulus of rutile is now determined less accurately (i.e., by ∼50 GPa lower to BLYP or PBE values and by ∼80 GPa to experiment) than the same property obtained using the parametrization set of Zheng et al.[19] (see Table 3).

To further validate our Ti−O parameters, we have also investigated the energetic characteristics of main low-index rutile surfaces. Table 4 gives the surface energies of (001) and (100) rutile calculated with SCC-DFTB in comparison to different DFT functionals within the slab approach. The surface energy E_{surf} is defined as the energy difference between the total energy of the slab (E_{slab}) and that of the regular crystal having the same number (n) of TiO_2 formula units (E_{bulk}) divided by twice the surface area (A) of the slab: $E_{surf} = (E_{slab} - nE_{bulk})/2A$. The calculated SCC-DFTB surface energy of the least stable (001) surface converges to 2.01 J/m^2 with the slab thickness that is slightly larger than the LDA result of Labat et al.[13] For the (100) surface, we observe small oscillations of the surface energy with the slab thickness reaching the final value of 1.192 J/m^2 that almost coincides with its LDA counterpart.[13] It should be noted that

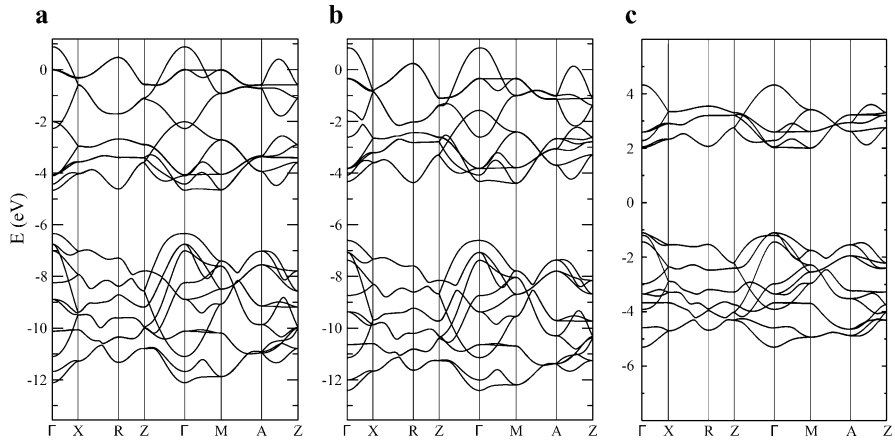

Figure 2. TiO_2 rutile band structures calculated with DFT-GGA using (a) PP I pseudopotential and (b) PP II pseudopotential, and (c) with current SCC-DFTB. For the description of PP I and PP II please refer to section 2.3.

Table 3. Comparison of the Geometric and Energetic Parameters of Bulk TiO_2 Rutile Structure Calculated with Different DFT Functionals, with SCC-DFTB Using Two Different Parametrization Sets, and Obtained from Experiment

				SCC-DFTB		
property	LDA[a]	PBE[a]	BLYP[a]	set of Zheng et al.[19]	current set	expt[b]
E_{coh}, eV	24.44	21.44	20.27	28.7	22.5	19.79
B_0, GPa	249	204	200	223	148	230 ± 20[c]
V_o, Å^3/TiO_2	30.2	31.8	32.7	33.0	32.8	31.217
a, Å	4.546	4.634	4.679	4.723	4.677	4.5936
c, Å	2.925	2.963	2.985	2.958	2.999	2.9587
c/*a*	0.643	0.639	0.638	0.626	0.641	0.6441
u	0.304	0.305	0.305	0.300	0.301	0.3048

[a] Literature values from ref 51; similar values were also reported by Labat et al.[13,53] for LDA and PBE functionals. [b] Structural parameters are taken from ref 85; cohesive energy E_{coh} is estimated on the basis of $\Delta H_f°(TiO_2,cr,298.15\ K) = -9.78$ eV,[1] $\Delta H_f°(O,g,298.15\ K) = 2.58$ eV,[1] and cohesive energy $E_{coh}(Ti,hcp)$ of 4.85 eV (cf. Table 2) as $E_{coh}(TiO_2) = E_{coh}(Ti) + 2\Delta H_f°(O,g,298.15K) - \Delta H_f°(TiO_2,cr,298.15K)$. [c] Literature value from ref 86.

Table 4. Comparison of the Energetics of Different Low-Index Surfaces of Rutile TiO_2[a]

(a) (001) surface

		E_{surf} for (001-13L) surface with other methods,[b] J/m^2				
n	E_{surf}(SCC-DFTB), J/m^2	HF	LDA	PBE	B3LYP	PBE0
4	1.887					
8	2.003	2.077	1.876	1.393	1.452	1.587
16	2.010					

(b) (100) Surface

		E_{surf} for (100-5L) surface with other methods,[b] J/m^2				
n	E_{surf}(SCC-DFTB), J/m^2	HF	LDA	PBE	B3LYP	PBE0
4	1.193					
8	1.176	1.128	1.197	0.694	0.699	0.833
16	1.192					

[a] Each slab contains *n* unit cells. [b] Literature values from ref 13.

the corresponding surface geometries agree well with their DFT analogues.

3.2.2. Properties of Anatase and Its Low-Index Surfaces. Figure 3 depicts the band structures of bulk anatase calculated with the hybrid HSE06[34,35] functional and SCC-DFTB. The indirect $\Gamma \rightarrow X$ band gap was found to be 3.7 and 3.2 eV with HSE06 and SCC-DFTB, respectively. The latter result is in a very close agreement with experimental band gap values of 3.2−3.3 eV.[52] The overall overestimation of band gaps with DFT using hybrid functionals is not surprising and was also reported earlier by Labat et al.[53] for the PBE0[54] functional. Unlike the rutile case, the SCC-DFTB band structure, apart from its compressed shape, reproduces well the main features of DFT band structure and is also in perfect agreement with experiment.

The main structural features and cohesive energies of bulk anatase calculated with DFT and SCC-DFTB together with experimental values are summarized in Table 5. With the current SCC-DFTB parametrization set, we obtain the cohesive energy of 22.3 eV/TiO_2. This value lies between the PBE result of Lazzeri et al.[51] of 21.5 eV and the hybrid HSE06[34,35] result of 22.9 eV. It should be noted that,

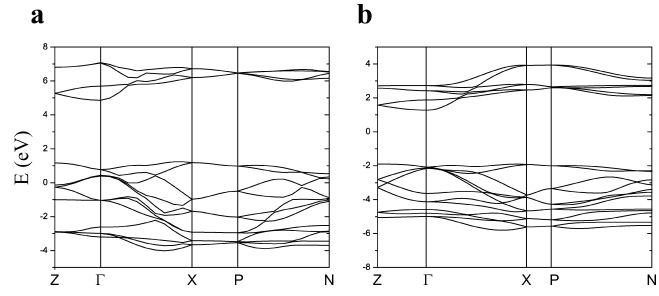

Figure 3. TiO_2 anatase band structures calculated with (a) HSE06 DFT functional and (b) SCC-DFTB with current parameters.

according to experimental observations,[53,55,56] rutile is the most stable TiO_2 polymorph and anatase should lie by up to 0.06 eV higher in energy than rutile. However, DFT functionals usually do not reproduce this stability order (except for LDA[53]). Surprisingly, the SCC-DFTB method gives the correct trend in stability with anatase being by 0.2 eV less stable than rutile and giving at the same time the

Table 5. Comparison of the Geometric and Energetic Parameters of Bulk TiO_2 Anatase Structure Calculated with Different DFT Functionals, with SCC-DFTB Using Two Different Parametrization Sets, and Obtained from Experiment

					SCC-DFTB		
property	LDA[a]	PBE[a]	BLYP[a]	HSE06[b]	set of Zheng et al.[19]	current set	expt[c]
E_{coh}, eV	24.46	21.54	20.39	22.90	28.41	22.3	19.73
B_0, GPa	199	176	178	−	60	133	179 ± 2[d]
V_o, Å^3/TiO_2	33.25	34.89	35.83	33.72	35.70	33.75	34.06
a, Å	3.735	3.786	3.828	3.752	3.914	3.801	3.7842
c, Å	9.534	9.737	9.781	9.578	9.322	9.346	9.5146
c/a	2.553	2.572	2.555	2.552	2.382	2.459	2.5143
u	0.207	0.206	0.206	0.206	0.216	0.214	0.2081

[a] Literature values from ref 51; similar values were also reported by Labat et al.[13,53] for LDA and PBE functionals. [b] This work. [c] Structural parameters are taken from ref 87; cohesive energy E_{coh} is estimated to be by up to 0.06 eV smaller than that of rutile (Table 3) after taking into account the difference in binding energies of rutile and anatase reported by Labat et al.[53] (or from the difference in their standard heats of formation[55]). [d] Literature value from ref 88.

Table 6. Comparison of the Energetics of Different Low-Index Surfaces of Anatase TiO_2[a]

(a) (001) Surface

		E_{surf} for (001-6L) surface with other DFT models,[b] J/m^2	
n	E_{surf} (SCC-DFTB), J/m^2	LDA unrelaxed/relaxed	PBE unrelaxed/relaxed
2, 4, 8	1.10	1.46/1.38	1.12/0.98

(b) (100) Surface

		E_{surf} for (100-6L) surface with other DFT models,[b] J/m^2		E_{surf} for (100-8L) surface with other methods,[c] J/m^2				
n	E_{surf} (SCC-DFTB), J/m^2	LDA unrelaxed/relaxed	PBE unrelaxed/relaxed	HF	LDA	PBE	B3LYP	PBE0
2	0.97							
4	0.96	1.90/0.96	1.59/0.58	1.024	0.971	0.625	0.666	0.732
8	0.97							

[a] Each slab contains n unit cells. [b] Literature values from ref 51. [c] Literature values from ref 13.

values of cohesive energy much closer to experiment than those from LDA calculations.

As concerns geometric parameters, LDA geometries reported by Lazzeri et al.[51] are the most accurate among the listed pure DFT functionals and GGA functionals tend to provide slightly larger lattice parameters of anatase. Much better results can be obtained if one utilizes a screened Hartree−Fock hybrid exchange-correlation functional, for instance, HSE06,[34,35] for which the lattice parameters differ from experiment by only 0.032 and 0.063 Å for a and c, respectively. Current SCC-DFTB parametrization results in an accurate value of a (see Table 5), though the c value is by 1.8% smaller than its experimental counterpart. The corresponding internal u parameter, which represents the ratio of apical Ti−O bond length to c, slightly exceeds the experimental value. Similar to the rutile case, the bulk modulus calculated with current SCC-DFTB parameters is underestimated by approximately 40−50 GPa to DFT and experiment but outperforms the set of Zheng et al.,[19] which gives a too low B_0 value (Table 5).

If one compares the surface energies of low-index anatase surfaces (see Table 6), one can easily see that the current SCC-DFTB parametrization yields the corresponding values of at least LDA quality: in the case of (001) surface, the SCC-DFTB result is between the LDA and PBE ones whereas for the (100) surface the SCC-DFTB result coincides with its LDA counterpart. The DFT stability order of these surfaces is also retained with SCC-DFTB.

3.2.3. Properties of Small Titanium Oxide Molecules. In the final step of verification of our SCC-DFTB Ti−O parameters with respect to DFT and to previous SCC-DFTB parameters of Zheng et al.,[19] we have investigated the geometric and energetic characteristics of small $(TiO)_n$ and $(TiO_2)_n$ molecules ($n = 1, 2$). The corresponding equilibrium geometries are given in Figure 4, whereas the total atomization energies are collected in Table 7.

The TiO molecule is the most well-characterized of all the systems presented in Figure 4, both experimentally and theoretically. It has a triplet ($^3\Delta$) ground state with an experimental bond length of 1.6202 Å[1] and atomization energy (D_0) of 158.4 ± 1.5 kcal/mol[57] that, after inclusion the zero-point-energy (ZPE) correction based on the experimental value of vibrational Ti−O frequency of 1009 cm^{-1},[1] leads to the electronic atomization energy (D_e) value of 159.8 ± 1.5 kcal/mol. Both B3LYP and SCC-DFTB slightly underestimate the equilibrium bond length for the same state with the maximum error of 0.033 Å to experiment while the same geometric parameter for the singlet state is described with SCC-DFTB more accurately (within 0.01 Å to DFT and 0.02 Å to experiment (1.602 Å)).[58] The cal-

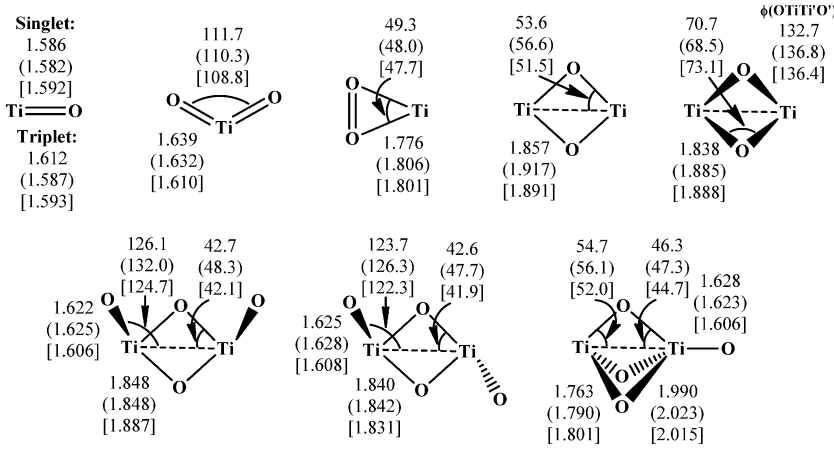

Figure 4. Schematic view of small isomeric $(TiO)_n$ and $(TiO_2)_n$ molecules ($n = 1, 2$) together with their equilibrium geometric parameters obtained with DFT (B3LYP/SDD+; without parentheses or brackets) and with SCC-DFTB using parameter set of Zheng et al.[19] (in parentheses) or using current set (in brackets).

Table 7. Total Atomization Energies[a] (TAEs, in kcal/mol) of Small Isomeric $(TiO)_n$ and $(TiO_2)_n$ Molecules ($n = 1, 2$) Calculated with DFT and SCC-DFTB

			SCC-DFTB	
molecule	point group, multiplicity	DFT[b]	set of Zheng et al.[c]	current set
TiO	$C_{\infty v}$, 1	135.9	208.7	190.9
	$C_{\infty v}$, 3	162.5	229.3	211.5
TiO_2	C_{2v}, 1	300.1	428.2	389.7
$Ti(O_2)$	C_{2v}, 1	199.7	284.5	243.0
Ti_2O_2	D_{2h}, 1	353.0	572.4	440.7
	C_{2v}, 1	385.3	582.2	453.3
Ti_2O_4	C_{2v}, 1	713.1	1002.8	862.5
	C_{2h}, 1	719.5	1005.8	865.2
	C_{3v}, 1	702.7	1015.8	825.5

[a] Total atomization energies refer to the energies of Ti and O atoms in their ground spin (triplet) states. [b] B3LYP/SDD+ (see section 2.3) calculations; this work. [c] Using the SCC-DFTB parameters of Zheng et al.;[19] this work.

culated SCC-DFTB atomization energies suffer from severe overbinding with the current parametrization leading to a by almost 0.8 eV lower value (9.17 eV) for ^{3}TiO in comparison to the set of Zheng et al.[19] (9.94 eV). The current SCC-DFTB atomization energy of ^{3}TiO is however comparable to the SVWN, SP86, and SLYP results reported earlier.[59] Interestingly, the excitation energies to the lowest-lying closed shell singlet ($^1\Sigma^+$) state of TiO are determined much closer to experiment with SCC-DFTB than with B3LYP leading to 0.89 eV (with both parametrization sets) and 1.15 eV, respectively, compared to the experimental value of 0.70 eV (5650 cm^{-1}).[60]

TiO_2 in its singlet ground state is known experimentally to have a bond length of 1.62 ± 0.08 Å (as quoted by Ramana and Philips[61]) and a bond angle of 110 ± 15°[62] from early IR measurements refined later to be 113 ± 5°.[63] The current SCC-DFTB parametrization reproduces well these geometric features of TiO_2 with an absolute error to DFT of 0.029 Å and 2.9° for the Ti−O bond length and O−Ti−O bond angle, respectively. It should be noted that, according to the recent high-level coupled-cluster CCSD/LANL2DZ calculations of Qu et al.[64] and CCSD(T)/aug-cc-pVTZ-PP ones of Li et al.,[65,66] the equilibrium bond length should be rather longer (1.672 and 1.666 Å, respectively) than the values commonly obtained by DFT using various functionals,[59] but the bond angle (112.6 and 112.4°) almost coincides with the best experimental estimate (see above) and is within 1° of our reference B3LYP value. The experimental $D_0(TiO_2)$ was reported to be 301.1 ± 2.9[67] and 304.0 ± 2.8 kcal/mol.[57] Because of lack of experimental values of the vibrational frequency for the O−Ti−O bending mode, it is not possible to calculate ZPE directly; therefore, a theoretical B3LYP/SDD+ ZPE correction of 3.4 kcal/mol is employed here leading to electronic atomization energies of 304.5 ± 2.9 and 307.4 ± 2.8 kcal/mol. Our reference DFT value of the TAE (300.1 kcal/mol) lies a few kilocalories per mole below the experimental estimates but agrees perfectly with the complete-basis-set extrapolated CCSD(T) value of 299.08 kcal/mol.[66] As in the case of TiO species, SCC-DFTB strongly overbinds TiO_2 with the current set being almost 90 kcal/mol above the reference DFT value.

Another TiO_2 isomer, cyclic peroxide $Ti(O_2)$, has been investigated only theoretically. Our reference DFT Ti−O bond length (1.776 Å) and O−Ti−O bond angle (49.3°) are in a good agreement with previous BLYP/6-311+G* results of Uzunova et al.[68] (1.785 Å and 48.8°, respectively) but lie slightly below the B3LYP/LANL2DZ results of Qu et al.[64] (1.814 Å and 50.9°). SCC-DFTB with current parameters reproduces well the geometric features of $Ti(O_2)$: the bond length deviates by 0.025 Å to DFT and the bond angle deviates by only 1.6°. The SCC-DFTB relative energies of singlet $Ti(O_2)$ with respect to the ground-state TiO_2 are determined however less accurately: B3LYP/SDD+ leads to the value of 4.35 eV (in accord with previous DFT results of 4.49 eV,[68] 4.73 eV[64]), whereas both SCC-DFTB parametrizations give 6.2−6.4 eV, indicating a different overestimation degree of pure metal oxide and metal peroxide bond energies.

According to DFT, dibridged cyclic Ti_2O_2 can exist as a planar D_{2h} or nonplanar ("butterfly") C_{2v} isomer with the latter being the global-minimum structure in agreement with previous calculations and experiment.[63,69,70] The SCC-DFTB optimized geometries are determined now with slightly larger errors when in the case of TiO and TiO_2 molecules: the bond

length can differ by up to 0.05−0.06 Å to B3LYP whereas bond angles may vary by ±3° to the same functional. It should be mentioned that our reference B3LYP geometric parameters depend also on the basis set size and the effective-core-potential versus all-electron approach, as exemplified by the B3LYP/6-311+G* Ti−O bond length in the D_{2h} isomer of 1.846 Å[69] that reduces the SCC-DFTB vs DFT bond length error to 0.042 Å. Although SCC-DFTB gives the correct stability order for these two Ti_2O_2 isomers, the actual SCC-DFTB relative energies are too low in comparison to our reference DFT value with the largest error of 22.5 kcal/mol represented by the set of Zheng et al.[19] Nevertheless, the current parametrization set now gives closer to DFT atomization energies per Ti−O bond (with the energy difference of about 17−22 kcal/mol) compared to TiO_2 (44.8 kcal/mol).

Three main isomeric structures were proposed for Ti_2O_4: cis dibridged (C_{2v}), trans dibridged (C_{2h}), and tribridged (C_{3v}) (cf. Figure 4)—with the lowest-energy isomer corresponding to the trans dibridged (C_{2h}) structure.[64,65,71,72] SCC-DFTB optimization with current parameters leads to a good agreement of geometric characteristics of these isomers with reference DFT data: the maximum error is 0.039 Å in bond lengths and 2.7° in bond angles. In addition, our reference DFT bond lengths agree within 0.023 Å to the recent CCSD(T)/aug-cc-pVTZ-PP results of Li et al.[65] The SCC-DFTB parametrization set of Zheng et al.[19] usually tends to give more open structures for these isomers with the bond angles much larger (up to 6°) compared to reference DFT values. In addition, the same set does not reproduce the correct stability order of Ti_2O_4 isomers (see Table 7), leading to C_{3v} isomer as the most stable one. The current parametrization set overcomes this discrepancy, but the relative SCC-DFTB energies of Ti_2O_4 isomers still differ significantly from their reference DFT and high-level ab initio counterparts: the cis dibridged (C_{2v}) lies by 2.7 kcal/mol higher in energy above the global minimum (compared to 6.4 kcal/mol with B3LYP/SDD+ or to 5.5 kcal/mol with CCSD(T)/CBS[65]), whereas the tribridged (C_{3v}) isomer is higher by almost 40 kcal/mol (compared to 16.8 kcal/mol with B3LYP/SDD+ or to 12.8 kcal/mol with CCSD(T)/CBS[65]). The total atomization energy of trans dibridged (C_{2h}) isomer derived experimentally at 0 K is 721.1 ± 11.2 kcal/mol[73] that, after including the ZPE (B3LYP/SDD+) correction of 9.1 kcal/mol, leads to the electronic atomization energy of 730.2 ± 11.2 kcal/mol. Our reference DFT value for the same isomer lies close to the lower bound of experimental estimate. The SCC-DFTB atomization energies are overestimated in all cases, but the overestimation degree of the current set is almost twice as low compared to that of Zheng et al.[19]

Overall, the current SCC-DFTB parametrization gives an acceptable description of small titanium molecules with geometric characteristics lying close to their DFT analogues. The total atomization energies are however overestimated for all the systems, and the relative energies between different isomers may vary significantly from their DFT analogues and should be treated with caution, especially if an unusual spatial arrangement of atoms is present.

3.3. Ti−H Interactions. As stated in Table 1, we have generated the repulsion profile of Ti−H interactions on the basis of the titane (TiH_4) molecule in its T_d symmetry using the cutoff value of 3.60 bohr. Table 8 lists total atomization energies together with equilibrium bond lengths and angles of TiH_x ($x = 1-4$) and dibridged C_{2v} Ti_2H_2 species. An inspection of these data reveals that the SCC-DFTB geometries of low-spin states are described quite accurately leading to the maximal Ti−H bond length error of 0.041 Å (for the singlet Ti_2H_2 case). Bond angles and dihedral angles are, however, the most sensitive parameters and may deviate up to 9.4° (for the singlet TiH_2 case) for low-spin systems in comparison to DFT values. This discrepancy usually originates from the very floppy profile of potential energy surfaces (PESs) associated with bending an angle or twisting a dihedral angle, on the one hand, or multireference character of the wave function that cannot be handled by single-reference methods without electron correlation, on the other. For example, the experimental value of the H−Ti−H angle of the ground ($^3B_1$) state of TiH_2 was found to be 145 ± 5°,[74] which is very far from our reference DFT and SCC-DFTB results. Moreover, its CISD/TZP(f,d) equilibrium geometry[75] is characterized by r(Ti−H) = 1.790 Å and α(H−Ti−H) = 142.1°, i.e., close to the experimental value. Demuynck and Schaefer[76] have predicted 10 possible electronic configurations of triplet TiH_2 in C_{2v} symmetry, some of which are low-lying. State-averaged CASSCF calculations of Kudo and Gordon[77] for the bent $^3B_1$ state lead to r(Ti−H) = 1.863 Å and α(H−Ti−H) = 140.7°, showing at the same time the corresponding floppy bending PES. A similar discrepancy is found for the lowest singlet

Table 8. Equilibrium Geometries and Total Atomization Energies[a] (TAEs) of Small Titanium Hydrides Calculated with DFT and SCC-DFTB Methods (r in Å, α and ϕ in deg, TAE in kcal/mol)

				SCC-DFTB	
molecule	spin multiplicity	parameter	DFT[b]	set of Zheng et al.[c]	current set
TiH	2	r	1.723	1.678	1.690
	2	TAE	49.5	51.4	49.2
	4	r	1.760	1.698	1.701
	4	TAE	59.5	83.2	81.2
TiH_2	1	r	1.696	1.690	1.696
	1	α	111.8	102.6	102.4
	1	TAE	98.1	117.7	113.2
	3	r	1.755	1.694	1.698
	3	α	121.9	104.8	105.1
	3	TAE	125.9	137.9	133.6
TiH_3 (D_{3h})	2	r	1.725	1.699	1.748
	2	TAE	185.8	197.8	172.1
TiH_4 (T_d)	1	r	1.685	1.688	1.695
	1	TAE	242.1	271.9	263.5
Ti_2H_2 (dibridged)	1	r(Ti−Ti)	1.988	2.082	1.967
	1	r(Ti−H)	1.868	1.865	1.827
	1	α(Ti−Ti−H)	57.9	56.1	57.4
	1	ϕ(H−Ti−Ti−H)	90.5	101.9	98.0
	1	TAE	152.1	261.9	229.5
	3	r(Ti−Ti)	2.020	2.096	1.975
	3	r(Ti−H)	1.875	1.836	1.812
	3	α(Ti−Ti−H)	57.4	55.2	56.9
	3	ϕ(H−Ti−Ti−H)	126.3	139.8	133.7
	3	TAE	154.0	260.5	224.0

[a] Total atomization energies refer to the energies of Ti and H atoms in their ground spin states (triplet and doublet, respectively). [b] B3LYP/SDD+ (see section 2.3) calculations; this work. [c] Using the SCC-DFTB parameters of Zheng et al.;[19] this work.

$^1A_1$ state of the bent TiH_2 with the CASSCF values of $r(Ti-H) = 1.899$ Å and $\alpha(H-Ti-H) = 168.4°$,[77] i.e., very different from our DFT and SCC-DFTB results. These observations clearly point out that our SCC-DFTB parametrization may not give the right answers in terms of geometries of triplet and singlet TiH_2 states as well as other high-spin states of titanium hydrides, having many low-lying electronic states and floppy bending PES profiles. It is interesting to note, however, that the SCC-DFTB triplet−singlet splitting (i.e., the energy difference between singlet and triplet) in TiH_2 was calculated to be 20.5 kcal/mol in excellent agreement with the state-averaged CASSCF result of 20.9 kcal/mol.[77]

For the total atomization energies (TAEs), the current SCC-DFTB parametrization generally yields more reasonable values close to their DFT analogues than the previous SCC-DFTB set.[19] In some cases, the SCC-DFTB TAEs however may differ by more than 1 eV from DFT as exemplified by the quartet TiH and both singlet and triplet Ti_2H_2 species. In addition, for planar TiH_3 radical we observe a different behavior of SCC-DFTB TAEs calculated with different parametrization sets with respect to the reference DFT one: the set of Zheng et al.[19] tends to overestimate TAE whereas our set underestimates TAE by almost the same amount as a result of different steepnesses of repulsion Ti−H profiles.

By comparing the high-spin → low-spin excitation energies (or splittings), one can see the correct performance of SCC-DFTB for TiH (4 → 2) and TiH_2 (3 → 1) species but the reverse behavior for the dibridged Ti_2H_2 (3 → 1) isomer, which is known to be triplet in its ground state.[78] This again indicates that the SCC-DFTB investigation of spatially strained systems, especially in their high-spin states, should be performed with caution.

3.4. Ti−C Interactions. As mentioned earlier, the Ti−C parameter set has been generated by using atomic parameters of carbon from the mio-set[16,17] and by applying a repulsion curve shift of 0.7 eV per Ti−C bond. To verify the applicability of this set for titanium−carbon compounds, we have performed a comparative investigation of the geometries and binding energies of one saturated $Ti(CH_3)_4$, one unsaturated $Ti(CH_3)_2$ molecule, and one complex of catalytic importance, $Ti(C_2H_4)^+$. The corresponding geometric characteristics together with total binding energies with respect to separate fragments (ligands) are presented in Table 9. The equilibrium geometry of $Ti(CH_3)_4$ agrees within 0.024 Å to DFT, and the binding energy is overestimated by 43.9 kcal/mol per four Ti−C bonds. Similar overestimation trends are also observed for $Ti(CH_3)_2$ species. However, new SCC-DFTB parameters result in much lower binding energies of $Ti(C_2H_4)^+$ complexes in comparison to their DFT analogues and to results of Zheng et al.[19] due to a much stronger contribution of repulsion energy to the total SCC-DFTB energy. Preliminary investigations indicate that it is possible to achieve the DFT-quality results for $Ti(C_2H_4)^+$ by applying smaller values for the repulsion curve shift; however, in such a case, the TAEs of covalently bound $Ti(CH_3)_4$ and $Ti(CH_3)_2$ systems will be overestimated by more than 1 eV per Ti−C bond that exceeds typical SCC-DFTB overbinding values found for other Ti−X systems as well as for test systems of mio-set.[16,17]

Table 9. Equilibrium Geometries, Binding Energies[a] (BEs), and High-Spin → Low-Spin Excitation Energies of Small Titanium−Carbon Compounds Calculated with DFT and SCC-DFTB Methods (r in Å, α in deg, BE in kcal/mol)

				SCC-DFTB	
molecule	spin multiplicity	parameter	DFT[b]	set of Zheng et al.[19]	current set
$Ti(CH_3)_4$	1	r	2.072	2.034	2.096
	1	BE	242.7	419.4	286.6
$Ti(CH_3)_2$	1	r	2.038	2.033	2.096
	1	α	113.7	110.1	110.2
	1	BE	98.1	192.4	125.4
	3	r	2.100	2.040	2.103
	3	α	122.1	117.6	118.4
	3	BE	118.2	209.9	143.0
	3 → 1	ΔE	20.1	17.5	17.6
$Ti(C_2H_4)^+$	2	r	2.029	1.993	2.015
	2	BE	68.0	99.9	35.0
	4	r	2.337	2.276	2.259
	4	BE	76.2	93.6	32.4
	4 → 2	ΔE	8.23	−6.26	−2.6

[a] BEs are defined as follows: for $Ti(CH_3)_n$, $BE = E(Ti) + nE(CH_3) - E(Ti(CH_3)_n)$; for $Ti(C_2H_4)^+$, $BE = E(Ti^+) + E(C_2H_4) - E(Ti(C_2H_4)^+)$. [b] B3LYP/SDD+ (see section 2.3) calculations; this work.

Table 10. Equilibrium Geometries and Binding Energies[a] (BE) of small Titanium−Nitrogen Compounds Calculated with DFT and SCC-DFTB Methods (r in Å, α in deg, BE in kcal/mol)

				SCC-DFTB	
molecule	spin multiplicity	parameter	DFT[b]	set of Zheng et al.[19]	current set
$Ti(NH_2)_4$ (S_4 symm)	1	r	1.899	1.874	1.902
	1	BE	358.9	383.5	361.6
H_3TiNH_2	1	r	1.846	1.859	1.898
	1	BE	91.6	104.5	118.0
HN=Ti=NH	1	r	1.707	1.692	1.703
	1	α	114.8	114.2	114.7
	1	BE	91.7	124.1	113.3

[a] BEs are defined as follows: for $Ti(NH_2)_4$, $BE = E(Ti) + 4E(NH_2) - E(Ti(NH_2)_4)$; for H_3TiNH_2, $BE = E(TiH_3) + E(NH_2) - E(H_3TiNH_2)$; for $Ti(NH)_2$, $BE = E(Ti) + E(N_2H_2) - E(Ti(NH)_2)$. [b] B3LYP/SDD+ (see section 2.3) calculations; this work.

It is worth noting that the SCC-DFTB high-spin → low-spin excitation energy for the $Ti(C_2H_4)^+$ complex has an opposite sign with respect to the DFT value. Such a result again confirms that the treatment of high-spin systems may not be adequate within the SCC-DFTB framework. Nevertheless, the current parametrization generally leads to an acceptable description of covalently bound titanium−carbon systems and may be applied further to molecules and bulk systems but may not give the right answer for charged coordination complexes, particularly, in their high-spin states.

3.5. Ti−N and Ti−S Interactions. Ti−N SCC-DFTB parametrization exemplifies another case where there was a need to shift the repulsion curve toward higher energies to diminish the degree of overbinding of reference systems (see Table 1). Table 10 contains the reference DFT and SCC-DFTB equilibrium geometries and binding energies of some small titanium−nitrogen-containing molecules. We can see

Table 11. Equilibrium Geometries and Total Binding Energies[a] (BEs) of Titanium Sulfides Calculated with DFT and SCC-DFTB Methods (r in Å, α in deg, BE in kcal/mol)

molecule	spin multiplicity	parameter	DFT[b]	SCC-DFTB[c]
TiS_2 (C_{2v})	1	r(Ti−S)	2.079	2.107
	1	α(S−Ti−S)	112.9	109.3
	1	BE	199.7	235.9
Ti_2S_3 (D_{3h})	1	r(Ti−S)	2.297	2.269
	1	BE	416.3	428.3
TiS ($C_{\infty v}$)	1	r(Ti−S)	2.021	2.007
	1	BE	82.6	113.8

[a] Total binding energy is calculated with respect to the energies of separate Ti and S atoms in their ground spin states. [b] B3LYP/SDD+ (see section 2.3) calculations; this work. [c] Current SCC-DFTB parametrization set.

that the current SCC-DFTB results almost coincide now with their DFT counterparts for the reference $Ti(NH_2)_4$ molecule. However, for another saturated compound, H_3TiNH_2, the current set gives a slightly larger Ti−N equilibrium bond length and binding energy. On the other hand, for the unsaturated $Ti(NH)_2$ compound, the current set is coming closer to the DFT values than the previous set.[19] Therefore, the current Ti−N set should be considered as generally applicable to model such systems and should not cause significant errors.

Finally, we have also performed the new SCC-DFTB parametrization of Ti−S interactions. Unlike the Ti−N case, for this pair of elements it was possible to apply a relatively large cutoff value in order to avoid the usage of the repulsion energy shift. The resulting SCC-DFTB parameters were tested against a few gas-phase titanium sulfides, and the obtained results are given in Table 11. It has been found that the reference TiS_2 molecule is characterized by only marginal Ti−S bond elongation as well as a small decrease of bond angle using the SCC-DFTB method in comparison to DFT. For other titanium sulfides tested, a small decrease in bond lengths (up to 0.028 Å) is observed. Concerning the total binding energies, the largest overbinding (of 36.2 kcal/mol) is found for the TiS_2 molecule whereas other sulfides are described with smaller absolute energy differences. Hence, the new SCC-DFTB set for titanium−sulfur interactions should yield relatively accurate equilibrium geometries of such sulfur-containing systems while slightly overbinding these compounds.

3.6. Water Splitting on (001) Anatase Surface: Test Case. It has been well established in the literature that the high reactivity of anatase nanoparticles should be associated with the minority (001) anatase surface,[79] which exhibited an unusually strong tendency to cause spontaneous water dissociation.[80,81] In turn, this high reactivity also originates from an unusual structural feature and high strain of the (001) surface, having two inequivalent Ti−O bonds and a large Ti−O−Ti bond angle.[51]

Vittadini et al.[81] have found three different adsorption modes for water adsorption on the (001) surface based on GGA calculations: dissociative, molecular, and mixed. Figure 5 depicts the corresponding local-minimum structures of adsorbed water on (001) anatase obtained with SCC-DFTB and DFT. Although we did not perform preliminary molecular dynamics simulations using different orientations of water molecules near the (001) surface in order to find more energetically preferable structures, but rather relied on the SCC-DFTB optimization itself, we were able to locate the main structures for these three modes with geometric characteristics close to their DFT analogues. The largest deviation in bond lengths has been found for the hydrogen-bonded −O···H distances that exceeded sometimes 0.4 Å in comparison to DFT ones, indicating that the corresponding potential energy surface may contain many close-lying minima not easily obtained through a simple energy minimization.

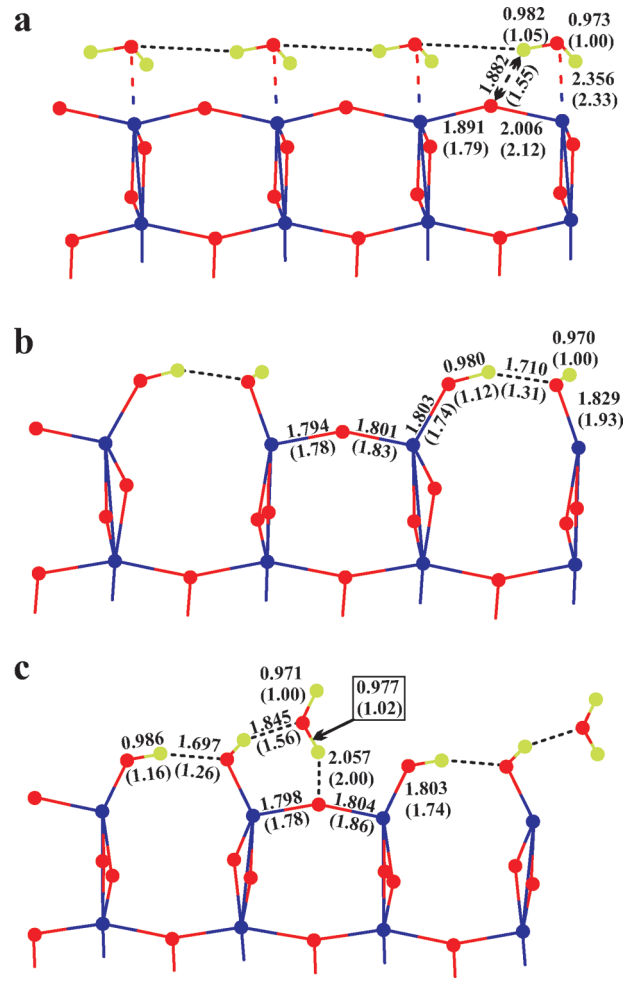

Figure 5. Structures of (001) anatase surfaces with adsorbed water molecules via (a) molecular, (b) dissociated, and (c) mixed adsorption modes. Bond lengths (in Å) without parentheses refer to SCC-DFTB ones obtained with current parametrization set, whereas those with parentheses are DFT values taken from Vittadini et al.[81] Titanium atoms are shown in blue, oxygen atoms are in red, and hydrogen atoms are in green. Hydrogen bonds are denoted with black dashed lines.

If one compares the energetic characteristics, i.e., adsorption energies per H_2O molecule, for different adsorption modes and capacities (shown in Table 12), one can also see a satisfactory agreement with DFT results of Vittadini et al.[81] SCC-DFTB also confirms that at coverages θ below 0.5 the dissociative mode is preferred over other modes whereas at $\theta > 0.5$ the mixed mode is more energetically favorable.

Table 12. Water Adsorption Energies (in eV/H_2O) on (001) Anatase Surface Calculated for the Different Adsorption Modes Using SCC-DFTB and DFT

adsorption mode	coverage,[a] θ	DFT[b]	SCC-DFTB[c]
molecular	0.5	0.81	0.66
	1	0.82	0.51
dissociative	0.5	1.44	1.59
mixed	1	1.01	0.96

[a] Coverage is defined as $n(H_2O)/n(5\text{-Ti})$, where $n(H_2O)$ and $n(5\text{-Ti})$ are the number of adsorbed water molecules and five-coordinated surface titanium atoms, respectively. [b] GGA results of Vittadini et al.[81] [c] Using current SCC-DFTB parametrization set.

Given the limitations of SCC-DFTB methods, on the one hand, and the difference in geometries for our SCC-DFTB and Vittadini et al.'s[81] DFT structures, on the other, the energy differences of 0.3 eV and smaller between SCC-DFTB and Vittadini et al.'s[81] corresponding DFT values should be considered as acceptable.

4. Conclusions

A new improved SCC-DFTB parametrization for titanium and its interactions with carbon, hydrogen, nitrogen, oxygen, and sulfur has been developed in order to get the best possible description of periodic and molecular systems involving these elements. This new SCC-DFTB set has been shown to give accurate values of the band gaps of the main TiO_2 polymorphs: rutile and anatase. The corresponding energetic and structural SCC-DFTB parameters of these bulk phases and their low-index surfaces are also in a good agreement with experimental and reference DFT results, outperforming the previous set of Zheng et al.[19] In addition, the careful generation of repulsion profiles for each pair of interacting elements allowed us to achieve much better binding (and/or atomization) energies of small molecular systems that generally lie close to their DFT counterparts and do not suffer from significant overbinding. However, it should be emphasized that the current SCC-DFTB set may rather not be applicable to small molecular systems in their high-spin states and with floppy potential energy surfaces or to systems whose wave functions exhibit significant multireference character. Nevertheless, the current set should serve as an excellent tool for the preliminary investigation of the adsorption of small molecules on rutile and anatase surfaces using considerably less computational resources as would be the case with ab initio methods.

When this work was finished, another SCC-DFTB parametrization involving titanium has been published by Luschtinetz et al.,[82] reporting structural and electronic characteristics of rutile and anatase bulk phases in a close agreement with our results. However, our set relies on the previously derived SCC-DFTB parameters for the first-row elements (mio-set) that have been shown[16−18,83] to perform well for many organic molecules and, therefore, this work should be considered as an attempt to generate the most suitable mio-based Ti−X (X = Ti, C, H, N, O, S) set to be applied to metal−organic compounds, to periodic (mainly, TiO_2) systems, and to systems involving small molecular adsorbates on rutile and/or anatase surfaces.

Acknowledgment. Mr. Huy Huynh Anh is gratefully acknowledged for performing HSE06 calculations for anatase using VASP software.

References

(1) Lide, D. R. *CRC Handbook of Chemistry and Physics*; CRC Press: Boca Raton, FL, 2005.

(2) Albrektsson, T.; Branemark, P. I.; Hansson, H. A.; Lindstrom, J. *Acta Orthop. Scand.* **1981**, *52* (2), 155–170.

(3) Jones, F. H. *Surf. Sci. Rep.* **2001**, *42* (3−5), 79–205.

(4) Corradini, P.; Guerra, G.; Cavallo, L. *Acc. Chem. Res.* **2004**, *37* (4), 231–241.

(5) Diebold, U. *Surf. Sci. Rep.* **2003**, *48* (5−8), 53–229.

(6) Buso, D.; Post, M.; Cantalini, C.; Mulvaney, P.; Martucci, A. *Adv. Funct. Mater.* **2008**, *18* (23), 3843–3849.

(7) Karunagaran, B.; Uthirakumar, P.; Chung, S. J.; Velumani, S.; Suh, E. K. *Mater. Charact.* **2007**, *58* (8−9), 680–684.

(8) Nazeeruddin, M. K.; Pechy, P.; Renouard, T.; Zakeeruddin, S. M.; Humphry-Baker, R.; Comte, P.; Liska, P.; Cevey, L.; Costa, E.; Shklover, V.; Spiccia, L.; Deacon, G. B.; Bignozzi, C. A.; Gratzel, M. *J. Am. Chem. Soc.* **2001**, *123* (8), 1613–1624.

(9) Fujishima, A.; Honda, K. *Nature* **1972**, *238* (5358), 37–38.

(10) Bannat, I.; Wessels, K.; Oekermann, T.; Rathousky, J.; Bahnemann, D.; Wark, M. *Chem. Mater.* **2009**, *21* (8), 1645–1653.

(11) Kalousek, V.; Tschirch, J.; Bahnemann, D.; Rathousky, J. *Superlattices Microstruct.* **2008**, *44* (4−5), 506–513.

(12) Menendez-Flores, V. M.; Friedmann, D.; Bahnemann, D. W. *Int. J. Photoenergy* **2008**; 280513/1-11.

(13) Labat, F.; Baranek, P.; Adamo, C. *J. Chem. Theory Comput.* **2008**, *4* (2), 341–352.

(14) Johnson, E. R.; DiLabio, G. A. *Chem. Phys. Lett.* **2006**, *419* (4−6), 333–339.

(15) Janowski, T.; Pulay, P. *Chem. Phys. Lett.* **2007**, *447* (1−3), 27–32.

(16) Elstner, M.; Porezag, D.; Jungnickel, G.; Elsner, J.; Haugk, M.; Frauenheim, T.; Suhai, S.; Seifert, G. *Phys. Rev. B* **1998**, *58* (11), 7260–7268.

(17) Porezag, D.; Frauenheim, T.; Köhler, T.; Seifert, G.; Kaschner, R. *Phys. Rev. B* **1995**, *51* (19), 12947–12957.

(18) Elstner, M.; Frauenheim, T.; Suhai, S. *J. Mol. Struct. (THEOCHEM)* **2003**, *632*, 29–41.

(19) Zheng, G. S.; Witek, H. A.; Bobadova-Parvanova, P.; Irle, S.; Musaev, D. G.; Prabhakar, R.; Morokuma, K.; Lundberg, M.; Elstner, M.; Köhler, C.; Frauenheim, T. *J. Chem. Theory Comput.* **2007**, *3* (4), 1349–1367.

(20) Elstner, M. *J. Phys. Chem. A* **2007**, *111* (26), 5614–5621.

(21) Perdew, J. P.; Burke, K.; Ernzerhof, M. *Phys. Rev. Lett.* **1996**, *77* (18), 3865–3868.

(22) Moreira, N. H.; Dolgonos, G.; Aradi, B.; da Rosa, A. L.; Frauenheim, T. *J. Chem. Theory Comput.* **2009**, *5* (3), 605–614.

(23) Becke, A. D. *J. Chem. Phys.* **1988**, *88* (2), 1053–1062.

(24) Lee, C. T.; Yang, W. T.; Parr, R. G. *Phys. Rev. B* **1988**, *37* (2), 785–789.

(25) Stephens, P. J.; Devlin, F. J.; Chabalowski, C. F.; Frisch, M. J. *J. Phys. Chem.* **1994**, *98* (45), 11623–11627.

(26) Dolg, M.; Wedig, U.; Stoll, H.; Preuss, H. *J. Chem. Phys.* **1987**, *86* (2), 866–872.

(27) Wedig, U.; Dolg, M.; Stoll, H.; Preuss, H. In *Quantum Chemistry: The Challenge of Transition Metals and Coordination Chemistry*; Veillard, A., Ed.; Reidel: Dordrecht, The Netherlands, 1986; Vol. 176, p 79.

(28) Frisch, M. J.; Pople, J. A.; Binkley, J. S. *J. Chem. Phys.* **1984**, *80* (7), 3265–3269.

(29) Frisch, M. J.; Trucks, G. W.; Schlegel, H. B.; Scuseria, G. E.; Robb, M. A.; Cheeseman, J. R.; Montgomery, J. A., Jr.; Vreven, T.; Kudin, K. N.; Burant, J. C.; Millam, J. M.; Iyengar, S. S.; Tomasi, J.; Barone, V.; Mennucci, B.; Cossi, M.; Scalmani, G.; Rega, N.; Petersson, G. A.; Nakatsuji, H.; Hada, M.; Ehara, M.; Toyota, K.; Fukuda, R.; Hasegawa, J.; Ishida, M.; Nakajima, T.; Honda, Y.; Kitao, O.; Nakai, H.; Klene, M.; Li, X.; Knox, J. E.; Hratchian, H. P.; Cross, J. B.; Bakken, V.; Adamo, C.; Jaramillo, J.; Gomperts, R.; Stratmann, R. E.; Yazyev, O.; Austin, A. J.; Cammi, R.; Pomelli, C.; Ochterski, J. W.; Ayala, P. Y.; Morokuma, K.; Voth, G. A.; Salvador, P.; Dannenberg, J. J.; Zakrzewski, V. G.; Dapprich, S.; Daniels, A. D.; Strain, M. C.; Farkas, O.; Malick, D. K.; Rabuck, A. D.; Raghavachari, K.; Foresman, J. B.; Ortiz, J. V.; Cui, Q.; Baboul, A. G.; Clifford, S.; Cioslowski, J.; Stefanov, B. B.; Liu, G.; Liashenko, A.; Piskorz, P.; Komaromi, I.; Martin, R. L.; Fox, D. J.; Keith, T.; Al-Laham, M. A.; Peng, C. Y.; Nanayakkara, A.; Challacombe, M.; Gill, P. M. W.; Johnson, B.; Chen, W.; Wong, M. W.; Gonzalez, C.; Pople, J. A. *Gaussian 03*, Revision B.04; Gaussian, Inc.: Wallingford, CT, 2004.

(30) Sánchez-Portal, D.; Ordejón, P.; Artacho, E.; Soler, J. M. *Int. J. Quantum Chem.* **1997**, *65* (5), 453–461.

(31) Soler, J. M.; Artacho, E.; Gale, J. D.; García, A.; Junquera, J.; Ordejón, P.; Sánchez-Portal, D. *J. Phys.: Condens. Matter* **2002**, *14* (11), 2745–2779.

(32) Kleinman, L.; Bylander, D. M. *Phys. Rev. Lett.* **1982**, *48* (20), 1425–1428.

(33) Troullier, N.; Martins, J. L. *Phys. Rev. B* **1991**, *43* (3), 1993–2006.

(34) Heyd, J.; Scuseria, G. E.; Ernzerhof, M. *J. Chem. Phys.* **2003**, *118* (18), 8207–8215.

(35) Vydrov, O. A.; Heyd, J.; Krukau, A. V.; Scuseria, G. E. *J. Chem. Phys.* **2006**, *125* (7), 224106/1-5.

(36) Blochl, P. E. *Phys. Rev. B* **1994**, *50* (24), 17953–17979.

(37) Kresse, G.; Joubert, D. *Phys. Rev. B* **1999**, *59* (3), 1758–1775.

(38) Kresse, G.; Furthmüller, J. *Phys. Rev. B* **1996**, *54* (16), 11169–11186.

(39) Kresse, G.; Furthmüller, J. *Comput. Mater. Sci.* **1996**, *6* (1), 15–50.

(40) Kresse, G.; Hafner, J. *Phys. Rev. B* **1993**, *47* (1), 558–561.

(41) Kresse, G.; Hafner, J. *Phys. Rev. B* **1994**, *49* (20), 14251–14269.

(42) Aradi, B.; Hourahine, B.; Frauenheim, T. *J. Phys. Chem. A* **2007**, *111* (26), 5678–5684.

(43) DFTB+ version 1.0 (p1); see http://www.dftb-plus.info (accessed Sept 30, 2009).

(44) Hestenes, M. R.; Stiefel, E. *J. Res. Natl. Bur. Stand.* **1952**, *49* (6), 409–436.

(45) Monkhorst, H. J.; Pack, J. D. *Phys. Rev. B* **1976**, *13* (12), 5188–5192.

(46) Philipsen, P. H. T.; Baerends, E. J. *Phys. Rev. B* **1996**, *54* (8), 5326–5333.

(47) Lu, Z. W.; Singh, D.; Krakauer, H. *Phys. Rev. B* **1987**, *36* (14), 7335–7341.

(48) Pascual, J.; Camassel, J.; Mathieu, H. *Phys. Rev. Lett.* **1977**, *39* (23), 1490–1493.

(49) Pascual, J.; Camassel, J.; Mathieu, H. *Phys. Rev. B* **1978**, *18* (10), 5606–5614.

(50) Kittel, C. *Introduction to Solid State Physics*, 7th ed.; John Wiley & Sons: New York, 1996; p 57.

(51) Lazzeri, M.; Vittadini, A.; Selloni, A. *Phys. Rev. B* **2001**, *6315* (15), 155409/1-9.

(52) Tang, H.; Berger, H.; Schmid, P. E.; Lévy, F.; Burri, G. *Solid State Commun.* **1993**, *87* (9), 847–850.

(53) Labat, F.; Baranek, P.; Domain, C.; Minot, C.; Adamo, C. *J. Chem. Phys.* **2007**, *126* (15), 154703/1-12.

(54) Adamo, C.; Barone, V. *J. Chem. Phys.* **1999**, *110* (13), 6158–6170.

(55) Fahmi, A.; Minot, C.; Silvi, B.; Causá, M. *Phys. Rev. B* **1993**, *47* (18), 11717–11724.

(56) Ranade, M. R.; Navrotsky, A.; Zhang, H. Z.; Banfield, J. F.; Elder, S. H.; Zaban, A.; Borse, P. H.; Kulkarni, S. K.; Doran, G. S.; Whitfield, H. J. *Proc. Natl. Acad. Sci. U.S.A.* **2002**, *99*, 6476–6481.

(57) Hildenbrand, D. L. *Chem. Phys. Lett.* **1976**, *44* (2), 281–284.

(58) Merer, A. J. *Annu. Rev. Phys. Chem.* **1989**, *40*, 407–438, and references therein.

(59) Bergström, R.; Lunell, S.; Eriksson, L. A. *Int. J. Quantum Chem.* **1996**, *59* (6), 427–443.

(60) Wu, H. B.; Wang, L. S. *J. Chem. Phys.* **1997**, *107* (20), 8221–8228.

(61) Ramana, M. V.; Phillips, D. H. *J. Chem. Phys.* **1988**, *88* (4), 2637–2640.

(62) McIntyre, N. S.; Thompson, K. R.; Weltner, J., W. *J. Phys. Chem.* **1971**, *75* (21), 3243–3249.

(63) Chertihin, G. V.; Andrews, L. *J. Phys. Chem.* **1995**, *99* (17), 6356–6366.

(64) Qu, Z. W.; Kroes, G. J. *J. Phys. Chem. B* **2006**, *110* (18), 8998–9007.

(65) Li, S. G.; Dixon, D. A. *J. Phys. Chem. A* **2008**, *112* (29), 6646–6666.

(66) Li, S. G.; Hennigan, J. M.; Dixon, D. A. *J. Phys. Chem. A* **2009**, *113* (27), 7861–7877.

(67) Balducci, G.; Gigli, G.; Guido, M. *J. Chem. Phys.* **1985**, *83* (4), 1909–1912.

(68) Uzunova, E. L.; Mikosch, H.; Nikolov, G. S. *J. Chem. Phys.* **2008**, *128* (9), 094307/1-12.

(69) Gong, Y.; Zhang, Q. Q.; Zhou, M. F. *J. Phys. Chem. A* **2007**, *111* (18), 3534–3539.

(70) Xiang, J.; Yan, X. H.; Xiao, Y.; Mao, Y. L.; Wei, S. H. *Chem. Phys. Lett.* **2004**, *387* (1−3), 66–69.

(71) Albaret, T.; Finocchi, F.; Noguera, C. *J. Chem. Phys.* **2000**, *113* (6), 2238–2249.

(72) Hagfeldt, A.; Bergstrom, R.; Siegbahn, H. O. G.; Lunell, S. *J. Phys. Chem.* **1993**, *97* (49), 12725–12730.

(73) Balducci, G.; Gigli, G.; Guido, M. *J. Chem. Phys.* **1985**, *83* (4), 1913–1916.

(74) Xiao, Z. L.; Hauge, R. H.; Margrave, J. L. *J. Phys. Chem.* **1991**, *95* (7), 2696–2700.

(75) Ma, B. Y.; Collins, C. L.; Schaefer, H. F. *J. Am. Chem. Soc.* **1996**, *118* (4), 870–879.

(76) Demuynck, J.; Schaefer, H. F. *J. Chem. Phys.* **1980**, *72* (1), 311–315.

(77) Kudo, T.; Gordon, M. S. *J. Chem. Phys.* **1995**, *102* (17), 6806–6811.

(78) Papai, I. *Theor. Chem. Acc.* **2000**, *104* (2), 131–139.

(79) Gong, X. Q.; Selloni, A. *J. Phys. Chem. B* **2005**, *109* (42), 19560–19562, and references therein.

(80) Vittadini, A.; Casarin, M.; Selloni, A. *Theor. Chem. Acc.* **2007**, *117* (5−6), 663–671.

(81) Vittadini, A.; Selloni, A.; Rotzinger, F. P.; Gratzel, M. *Phys. Rev. Lett.* **1998**, *81* (14), 2954–2957.

(82) Luschtinetz, R.; Frenzel, J.; Milek, T.; Seifert, G. *J. Phys. Chem. C* **2009**, *113* (14), 5730–5740.

(83) Niehaus, T. A.; Elstner, M.; Frauenheim, T.; Suhai, S. *J. Mol. Struct. (THEOCHEM)* **2001**, *541*, 185–194.

(84) Da Silva, J. L. F.; Stampfl, C.; Scheffler, M. *Surf. Sci.* **2006**, *600* (3), 703–715.

(85) Abrahams, S. C.; Bernstein, J. L. *J. Chem. Phys.* **1971**, *55* (7), 3206–3211.

(86) Gerward, L.; Olsen, J. S. *J. Appl. Crystallogr.* **1997**, *30*, 259–264.

(87) Horn, M.; Schwerdtfeger, C. F.; Meagher, E. P. *Z. Kristallogr.* **1972**, *136* (3−4), 273–281.

(88) Arlt, T.; Bermejo, M.; Blanco, M. A.; Gerward, L.; Jiang, J. Z.; Olsen, J. S.; Recio, J. M. *Phys. Rev. B* **2000**, *61* (21), 14414–14419.

CT900422C